IEEE Access
Multidisciplinary | Rapid Review | Open Access Journal

Received September 11, 2019, accepted September 24, 2019, date of publication October 14, 2019,
date of current version October 25, 2019.

Digital Object Identifier 10.1109/ACCESS.2019.2947215

Wideband Transition for Increased-Height Empty Substrate Integrated Waveguide

JUAN A. MARTÍNEZ[1], ANGEL BELENGUER[1], (Senior Member, IEEE), JUAN J. DE DIOS[1], HÉCTOR ESTEBAN GONZÁLEZ[2], (Senior Member, IEEE), AND VICENTE E. BORIA[2], (Fellow, IEEE)

[1]Departamento deIngeniería Eléctrica, Electrónica, Automática y Comunicaciones, Escuela Politécnica de Cuenca, Universidad de Castilla-La Mancha, Campus Universitario,16071 Cuenca, Spain
[2]Departamento de Comunicaciones, Universitat Politècnica de València, 46022 Valencia, Spain

Corresponding author: Angel Belenguer (angel.belenguer@uclm.es)

This work was supported in part by the Ministerio de Economía y Competitividad, Spanish Government, under Project TEC2016-75934-C4-3-R and Project TEC2016-75934-C4-1-R, and in part by the Consejería de Educación, Cultura y Deportes, Autonomous Government of Castilla-La Mancha, under Project SBPLY/17/180501/000351.

ABSTRACT Recently, Empty Substrate Integrated Waveguide (ESIW) technology was proposed for embedding empty waveguides into planar substrates in order to improve their performance. A low-loss and narrow-band transition from microstrip to an increased height ESIW with 4 layers was presented in a previous work, and used to implement a very high-quality factor bandpass filter at Q-band. With such a narrow-band transition, based on a quarter-wavelength transformer, a very narrow-band filter response with resonators having a quality factor of 1000 was achieved. In this paper, in order to overcome the narrow-band and the 4-layers output restrictions, and extend the practical use of such increased height ESIWs beyond narrow-band filters, we present a novel wideband transition from microstrip to an increased height ESIW with an arbitrary number of layers. A full suite of wideband transitions to increased height ESIWs, built with different number of substrate layers ranging from 3 to 8, has been designed in this work to operate at Ka-band, though they can be easily transferred to other bands if the dimensions of the transition are properly scaled. To illustrate this, the original Ka-band transitions have been mapped to Ku-band, with excellent results. In order to test the proposed design method, a prototype of a 4-layer structure has been fabricated at Ka-band, achieving a good performance in the whole useful bandwidth of the ESIW.

INDEX TERMS Empty substrate integrated waveguide, ESIW, high quality factor, microstrip transition, multilayer, substrate integrated circuit, SIC, substrate integrated waveguide, SIW.

I. INTRODUCTION

Over the last few years, several technologies have been proposed for the implementation of Substrate Integrated Circuits (SICs), in order to merge planar and non-planar structures for achieving high-performance integrated devices used in high-frequency applications. Substrate Integrated Waveguide (SIW) [1] is among the most popular technologies developed for the integration of non-planar waveguides in Printed Circuit Boards (PCBs). Its low cost, ease of manufacture, and small size are the main advantages of SIW technology for the integration within PCBs. Although SIW provides better performance than traditional planar circuits, the substrate losses increase the total insertion loss and reduce its quality factor, especially at high frequencies.

Since 2014, several alternatives of Empty SICs [2]–[7] have been proposed in order to reduce losses in SIC devices by eliminating the dielectric substrate. Among them, the Empty Substrate Integrated Waveguide (ESIW) [2] shows a very good performance, since the dielectric is completely removed, and, as a result, total losses are decreased, while maintaining the advantages of SIWs about low cost, low profile, easy manufacturing and integration in a PCB. Due to the absence of dielectric, ESIW-based devices are not so compact as their equivalent SIW circuits. However, as frequency increases, the outperformance of the ESIW in terms of loss and quality factor gradually becomes more significant. The improvement that can be achieved with ESIWs could be even more significative if a practical way to further

The associate editor coordinating the review of this manuscript and approving it for publication was Wenjie Feng.

increase the quality factor of related devices is found. In fact, in [8], a multilayer transition was proposed to integrate ESIW guides with four times the height of the substrate holding the planar feeding lines. However, the proposed transition can efficiently feed an ESIW in a narrow bandwidth, so that it can only be used for integrating narrow-band components such as highly selective filters. Therefore, in this paper, a new wideband transition for integrating increased-height ESIWs is proposed in order to overcome the present narrow-band restriction, and extend the practical use of such increased-height ESIWs beyond narrowband filters. This new wideband transition covers the entire useful mono-mode bandwidth of the integrated ESIW and, as a result, can be used to integrate wideband devices in full bandwidth applications. Besides, this new transition can be used to feed increased-height ESIWs composed by an arbitrary number of layers. That is, with this novel transition, it is possible to choose the quality factor of the integrated devices, since the number of layers of the integrated increased-height ESIW can be increased or decreased as needed in the design stage (this is not possible if the transition of [8] is used).

Another important advantage of this novel transition is that it can be scaled to different frequency bands from a single design at a certain frequency. To prove this, a full set of transitions at Ku-band has been mapped from previous designs at Ka-band, by simply scaling its dimensions. A back-to-back prototype for this kind of transitions, operating at Ka-band, has been successfully designed, fabricated, and measured. The achieved experimental results show a good performance of the manufactured prototype. Therefore, the main goal of this work has been achieved, since the first known wideband transition between ESIWs of different height has been proposed and experimentally validated.

This paper is structured as follows: the transition between ESIWs of different heights for broadband applications, and its design procedure, is proposed in section II. In section III, the design of a set of transitions for Ka-band is detailed. The frequency scaling of the proposed design method is discussed in section IV, where it is successfully applied to deduce another set of transitions for Ku-band. The measured results for the manufactured prototype of the novel transitions at Ka-band are analyzed and compared with simulations in section V. Finally, the main conclusions of this work are discussed in section VI.

II. WIDEBAND TRANSITION BETWEEN ESIWS OF DIFFERENT HEIGHT

In a classical rectangular waveguide, when the height of the waveguide needs to be changed, a multi-section quarter-wavelength transformer is commonly used. The first idea is to directly transfer this traditional waveguide solution to ESIW. Unfortunately, there is an important difference between a classical waveguide and an ESIW. In classical rectangular waveguides, we can manufacture a waveguide of arbitrary height, but this is not possible for ESIWs. Since ESIWs are built using a stack of substrate layers, only a discrete set of heights is possible [8]. If we truncate the classical transformer heights to the nearest discrete height available in a multilayer ESIW, the resulting transformer exhibits very poor performance. Therefore, we must find an alternative high-performance solution, i.e. with high return loss, that allows the change in height in a multilayer ESIW, where the practicable heights are discrete. We have achieved this goal by modifying the geometry of the guide at each step of the quarter-wavelength transformer. In other words, we have not used rectangular waveguides to implement the transformer.

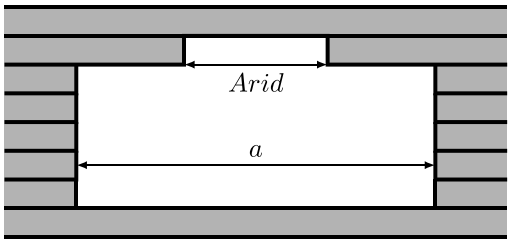

FIGURE 1. Cross-section view of the waveguide used to implement the intermediate steps of the height transformer in ESIW.

The ESIW transformer has been designed based on an equivalent transformer in classical rectangular waveguide, that is, with input and output waveguides of the same height as the input and output ESIWs. This classical transformer, though with identical input and output waveguides, shows intermediate steps of arbitrary height, which are unfeasible in a multilayer ESIW. Therefore, each step of the transformer has been replaced by a waveguide with a non-rectangular cross-section. This non-rectangular waveguide can be implemented using only the discrete available heights, and exhibits the same impedance as the original waveguide, i.e. when this waveguide is fed with the previous step in the transition, the resulting reflection coefficient is the same one that is obtained in the same position in the classical equivalent transformer.

To integrate the increased-profile ESIW devices, a suitable transition to classical planar lines is needed. The whole transition is then composed by the cascade connection of the microstrip to ESIW transition of [9], and the quarter-wavelength transformer described in the previous paragraph.

A. INTERMEDIATE GUIDES

As advanced in the previous section, the discrete nature of the available heights in a multilayer ESIW causes that the impedance of the intermediate guides in a typical waveguide height transformer cannot be precisely adjusted. In order to recover the required fine control of the impedance in the intermediate waveguides, the cross-section of the guide is modified. In Fig. 1, one can see the proposed new geometry for the cross-section of intermediate waveguides. This modified geometry adds an additional layer with reduced width ($Arid$) to a typical rectangular cross-section of width (a). In this way, when this extra-layer width ($Arid$) is modified, the impedance of the waveguide can be fine-tuned. The impedance of a modified waveguide of N layers, ranges from the impedance

of a rectangular waveguide of width a and $N-1$ layers ($Arid = 0$), to the impedance of a rectangular waveguide of the same width (a) and N layers ($Arid = a$). Therefore, the required fine control of the impedance is achieved for these multilayer-based integrated waveguides. Although, strictly speaking, the impedance can be controlled only with $Arid$, with this single parameter tuning, the impedance can be exactly adjusted only at a single frequency. In order to provide a wideband impedance control, another parameter should be involved. Therefore, the width of the base waveguide of Fig. 1, a, is also varied to modify the impedance of the waveguide, so that a more stable value is achieved in the whole bandwidth of interest. This happens because if only $Arid$ is used, the cutoff frequency of the waveguide is modified. As a result, the impedance dependence with frequency is different for input and output waveguides and, as a result, the reflection coefficient at the transition shows a non-despicable dependence with frequency. If the width of the base waveguide is modified accordingly with $Arid$, the cutoff frequency of the feeding waveguides can be recovered, so that the reflection coefficient exhibits a more stable response with frequency. Therefore, the main width of each step of the transition (a_i) is, in general, different. As a result, the transition in the main ESIW layer (the one supporting the microstrip feedings), shows the aspect depicted in Fig. 2(a). The geometry of the other layers can be seen in figures 2(b) and 2(c).

For example, the first step of a four-step transition in Ka-band from 1 to 8 layers goes from 1 layer (input) to 2 layers. If this transtion were implemented using a traditional multisection transformer, the reflection coefficient for this step would be equal to -20.5777 dB. Therefore, in the real ESIW transition, this first step has been designed to provide this same reflection coefficient. However, in this example, in order to illustrate that both a and $Arid$ should be modified, two different steps have been designed. In the first design, only $Arid$ has been optimized to achieve the desired impedance mismatch (the required S_{11}). In the second design, both a and $Arid$ have been modified to obtain, again, the desired S_{11}, but preserving the cutoff frequency of the feeding rectangular waveguides. In Fig. 3, the results for both designs are shown, and they prove that adjusting both a and $Arid$ provides a better impedance match in the whole bandwidth of interest (S_{11} and S_{21} almost constant with frequency).

B. DESIGN PROCEDURE

The transition is composed, in general, of an input waveguide of one layer and an output waveguide of N layers. To design this transition the following procedure can be applied:

1) The equivalent rectangular waveguide ideal transformer of N_e steps is designed, for the whole useful bandwidth of the guide [10].
2) The arbitrary heights of the intermediate steps are rounded to the nearest and lower discrete height, thus obtaining N_i, the number of layers of the base waveguide for each step of the transformer.

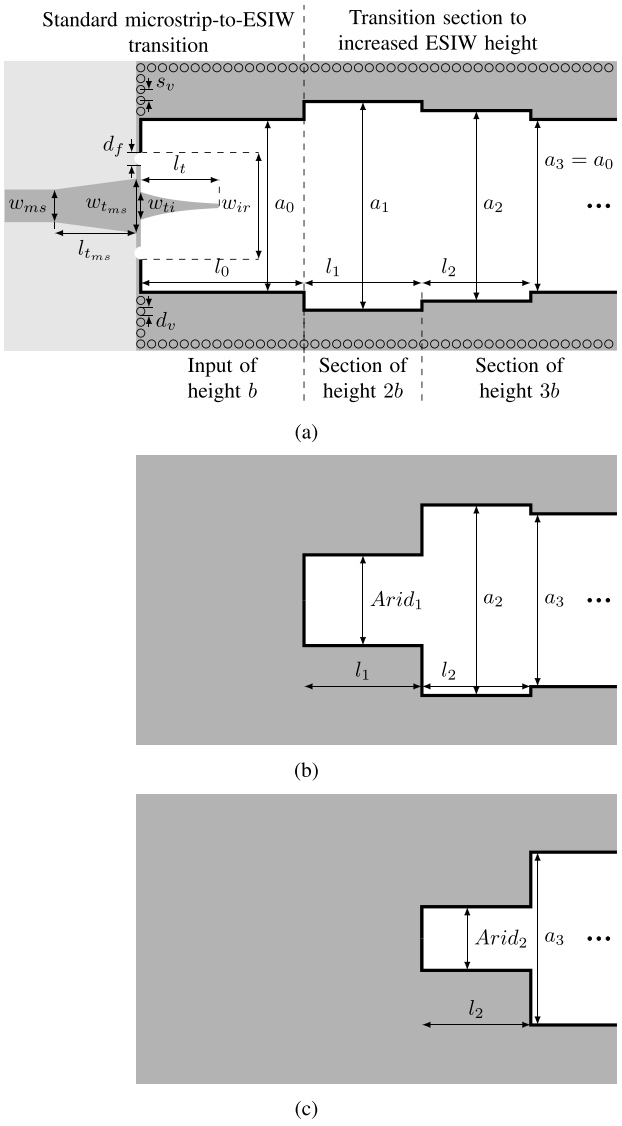

FIGURE 2. Transition with 2 steps from microstrip to an ESIW of 3 layers. Light gray: dielectric substrate. Dark gray: copper metallization on top layer. Black: border metallization used to close the ESIW. White: air. Top view of (a) main layer, (b) second layer, (c) third layer. Cover layers not shown.

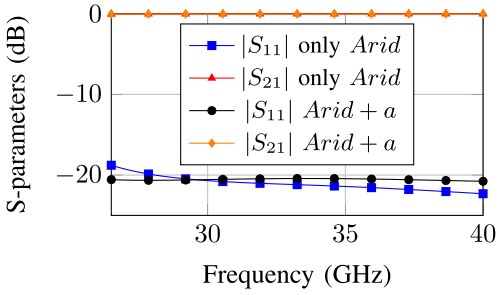

FIGURE 3. Comparison of simulations only optimizing ***Arid***, and both, ***Arid*** and ***a***.

3) Since the height of the waveguide is smaller than in the reference transformer, one layer is added to each step. However, to recover the impedance of the waveguide of

the reference transformer, the width in this extra layer ($Arid_i$) is smaller than the width of the rest (a_i). When the extra layer of reduced width is added, the cutoff frequency of the resulting waveguide shifts away from the original cutoff frequency of the rectangular waveguide of the ideal transformer. As a result, the response of every jump in the transformer can be well adjusted only at a single frequency (see discussion in previous section). In order to recover an almost frequency independent response of the jump, the width of the base waveguide (a_i) must be also modified, so that the cutoff frequency of the intermediate waveguides coincides with the cutoff frequency of the feeding rectangular waveguides. In order to obtain the transversal dimensions of the intermediate waveguides, $Arid_i$ and a_i, two empirical formulas have been deduced. First, the following expression is proposed to calculate $Arid_i$:

$$Arid_i = a\left(\frac{\hat{b}_i}{\hat{b}_0} - N_i\right), \quad \text{with } i = 1, 2, \ldots N_e \quad (1)$$

being: $Arid_i$ the width of the extra layer in the i-th step of the transformer, N_e the number of steps in the transformer, $\hat{b}_i$ the height of the i-th step of the equivalent transformer in rectangular waveguide, $\hat{b}_0$ is the height of a single layer, i.e. the height of the transformer feeding waveguide, a the width of the feeding waveguides, and N_i is the number of layers of the base waveguide in the i-th step of the transformer. With regard to the modified value for the width of each base waveguide (i.e. a_i), we make use of the next empirical expression:

$$a_i = a\left[1 + K_i\left(\frac{\alpha_i + (Arid_i/a)^{\beta_i}}{\alpha_i + (Arid_i/a)^{\gamma_i}} - 1\right)\right] \quad (2)$$

where:

$$\begin{aligned} i &= 1, 2, \ldots N_e \\ K_i &= \frac{6.2019}{N_i} + 0.0257 \\ \alpha_i &= 36.6404e^{-1.5807*N_i} + 1.3829 \\ \beta_i &= 1.5761(1 - e^{-1.0055*N_i}) + 0.3830 \\ \gamma_i &= 8.7830e^{-2.3936*N_i} + 2.3353 \end{aligned} \quad (3)$$

4) For each jump, the phase of the reflection coefficient at the input ($Ph(S_{11})$) and output ($Ph(S_{22})$) ports are calculated using CST Microwave Studio. The reference plane for this phase calculation must coincide with the plane of the jump. Due to the increasing impedance in each step, theoretically $Ph(S_{11}) = 0$ and $Ph(S_{22} = \pi)$. Then, a pair of length correction to obtain the required phase are calculated in each step ($i = 1, 2, \ldots N_e + 1$). In the input port of the i-th jump:

$$\Delta\ell_i^{(11)} = \frac{Ph^{(i)}(S_{11})}{2\beta_{i-1}}, \quad i = 1, 2, \ldots N_e + 1 \quad (4)$$

where $Ph^{(i)}(S_{11})$ is the i-th jump imput reflection coefficient phase between $[-\pi, \pi]$ and β_{i-1} is the phase constant in the input waveguide at the bandwidth central frequency. In the output port:

$$\Delta\ell_i^{(22)} = \frac{Ph^{(i)}(S_{22}) - \pi}{2\beta_i}, \quad i = 1, 2, \ldots N_e + 1 \quad (5)$$

where $Ph^{(i)}(S_{22})$ is the output reflection coefficient phase within the interval $[0, 2\pi]$, and β_i is the output waveguide phase constant at the central frequency of the bandwidth. Then, the length of the i-th intermediate waveguide is:

$$\ell_i = \lambda_{gi}/4 + \Delta\ell_i^{(22)} + \Delta\ell_{i+1}^{(11)}, \quad i = 1, 2, \ldots N_e \quad (6)$$

where λ_{gi} is the guided wavelength of the i-th intermediate waveguide at the central frequency of the transformer bandwidth.

5) A final optimization is executed. The final device is composed by cascading all the steps. The parameters a_i, $Arid_i$ and ℓ_i are again optimized (this time all of them from $i = 1$ to N_e at the same time) to minimize the reflection coefficient in the whole bandwidth of interest using the Trust Region Framework algorithm provided by CST Microwave Studio.

TABLE 1. Dimensions of the microstrip to ESIW transition.

Parameter	Value (mm)	Parameter	Value (mm)
a_0	7.1120	$1/c$	1.4404
l_0	5.0000	w_{ir}	3.2622
h	0.3050	w_{ti}	1.3172
w_{ms}	0.6200	l_t	2.8171
w_{tf}	0.2500	$w_{t_{ms}}$	0.9059
d_f	0.5000	$l_{t_{ms}}$	1.8523
d_v	0.5000	s_v	0.8000

III. TRANSITION DESIGN IN KA-BAND

In order to design the wideband transition, the previously described process is followed. A set of transitions, with different heights of the output waveguide, are designed to operate at Ka-band, and are implemented using a Rogers 4003C substrate of height $h_c = 0.305$ mm, permittivity $\epsilon_r = 3.55$, and metal thickness $t = 26.5\ \mu m$ (considering both original and galvanic metallizations), so that the height of a single layer ESIW is $b = 0.358$ mm (see Fig. 2(a)). Cover layers of FR-4 of height $h = 1\ mm$, and identical metallization, are used to enclose the device.

A. TRANSITION TO A 5-LAYER OUTPUT ESIW

A transition to a 5-layer height output ESIW, consisting of a structure with 3 steps and 4 impedance jumps, will be considered in order to explain the design process. The phases 1 to 4 described in subsection II-B will be followed in order to design the height transformer. The first part of the transition is a standard microstrip to ESIW transition; it is designed using [9] and adapted to our substrate. Its dimensions (see first part of Fig. 2(a)) can be seen in Table 1.

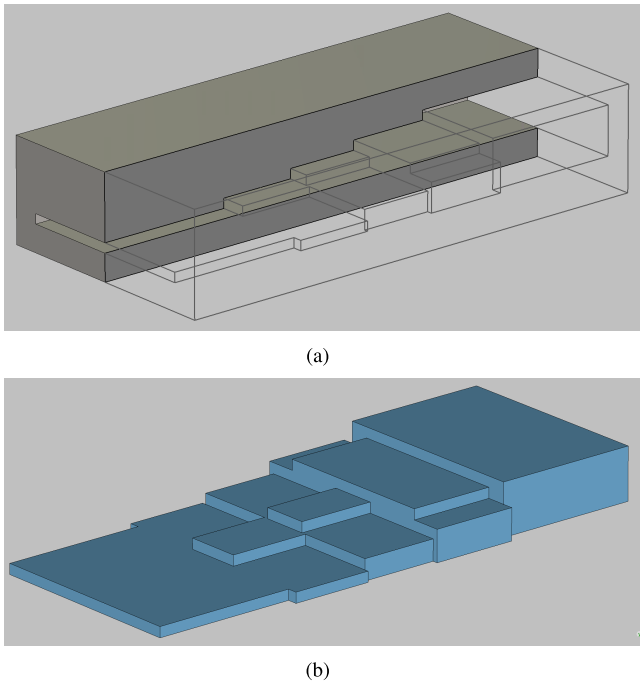

FIGURE 4. 5-layer transformer structure after optimization. (a) Cross-section view, showing the empty inner part of the ESIW device. (b) Blue-colored representation of the air-filled volume inside the transition.

TABLE 2. Initial dimensions of the whole set of transitions at Ka-band ($a_1 = 7.112$ mm).

	Value (mm)					
Param.	3-layer	4-layer	5-layer	6-layer	7-layer	8-layer
a_1	8.1718	7.7799	7.9315	8.0559	8.1589	7.6368
a_2	7.3529	7.1120	7.4813	7.8437	7.9028	7.1120
a_3	-	7.3268	7.4427	7.5405	7.1464	7.1120
a_4	-	-	-	-	-	7.3966
l_1	3.0232	2.9681	2.8554	2.7714	2.7698	2.9299
l_2	2.7784	2.7248	2.7895	2.8200	2.9038	2.7134
l_3	-	3.0399	3.0071	3.0686	2.7458	2.6622
l_4	-	-	-	-	-	3.2084
$Arid_1$	1.3532	0.8922	1.0619	1.2077	1.3363	0.7341
$Arid_2$	0.6154	0	0.8395	1.5984	2.2963	0
$Arid_3$	-	0.7031	3.0233	1.7029	0.3130	0
$Arid_4$	-	-	-	-	-	2.2440

The second part of the transition is intended to increase the ESIW height, as can be seen in Fig. 2(a). In this case, the device consists of 3 steps.

The complete structure is represented in Fig. 4, in particular the empty inner part of the ESIW device, and then it has to be optimized using the procedure described in phase 5. The initial and final dimensions after this optimization process, using the Trust Region Reflective algorithm in CST Microwave Studio, are shown in the fourth column of Table 2 and Table 3, respectively.

The scattering parameters of the complete height transformer, simulated with CST Microwave Studio in a frequency range from 26.5 to 40 GHz, are represented in Fig. 5.

TABLE 3. Optimized dimensions of the whole set of transitions at Ka-band ($a_0 = 7.112$ mm, $b = 0.358$ mm).

	Value (mm)					
Param.	3-layer	4-layer	5-layer	6-layer	7-layer	8-layer
a_1	8.4292	7.8218	8.1511	8.2835	8.4933	7.2495
a_2	7.4944	7.1120	7.5345	8.0510	8.6929	7.1120
a_3	-	7.2503	7.9472	7.8098	7.2897	7.1120
a_4	-	-	-	-	-	8.0135
l_1	2.9111	2.9625	2.7811	2.6529	2.5311	2.9809
l_2	2.7786	2.7280	2.7002	2.7381	2.9311	2.6646
l_3	-	3.0605	2.9791	3.0430	2.7580	2.5556
l_4	-	-	-	-	-	2.9749
$Arid_1$	1.2818	0.9024	1.0413	1.1960	1.3205	0.6746
$Arid_2$	0.6314	0	0.8026	1.5472	2.0820	0
$Arid_3$	-	0.7033	2.8658	1.6619	0.3265	7.1120
$Arid_4$	-	-	-	-	-	2.4684
	Number of layers					
	3-layer	4-layer	5-layer	6-layer	7-layer	8-layer
Step 1	2	2	2	2	2	2
Step 2	3	3	3	3	3	3
Step 3	-	4	4	5	5	4
Step 4	-	-	-	-	-	7

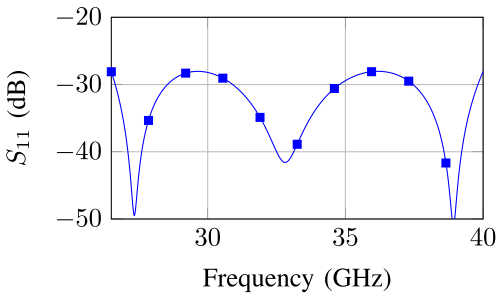

FIGURE 5. Simulated results of the designed transition to a 5-layer ESIW at Ka-band.

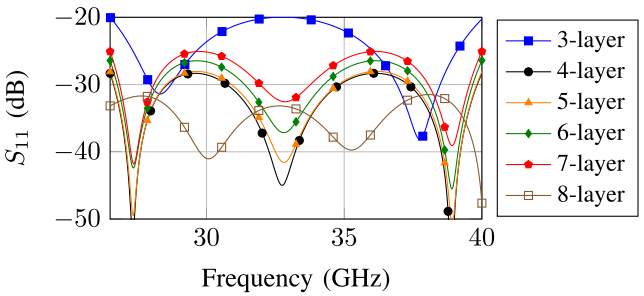

FIGURE 6. Simulation results of all the designed transitions at Ka-band.

B. N-TH LAYER TRANSITIONS

The same procedure can be applied for an output waveguide with an arbitrary number of layers. We have designed, applying the proposed design method, transitions from an input ESIW of 1 layer of height, to output ESIWs with heights ranging from 3 to 8 layers. The parameters obtained after the last full optimization step are listed in Table 3 for all the designed transformers.

The scattering parameters of the transformers are represented in Fig. 6 in the frequency range from 26.5 to 40 GHz (40% fractional bandwidth).

TABLE 4. Dimensions of the whole set of transitions at Ku-band ($a_0 = 15.7988$ mm, $b = 0.866$ mm).

	Value (mm)					
Param.	3-layer	4-layer	5-layer	6-layer	7-layer	8-layer
a_1	18.725	17.376	18.107	18.401	18.867	16.104
a_2	16.648	15.799	16.738	17.885	19.311	15.799
a_3	-	16.106	17.654	15.799	16.194	15.799
a_4	-	-	-	-	-	17.801
l_1	6.4669	6.5810	6.1781	5.8932	5.6227	6.6219
l_2	6.1724	6.0600	5.9983	6.0825	6.5113	5.9194
l_3	-	6.7987	6.6179	6.7598	6.1269	5.6772
l_4	-	-	-	-	-	6.6086
$Arid_1$	2.8475	2.0047	2.3132	2.6570	2.9334	1.4987
$Arid_2$	1.4026	0	1.7829	3.4371	4.6250	0
$Arid_3$	-	1.5624	6.3661	3.6919	0.7254	15.799
$Arid_4$	-	-	-	-	-	5.4833
	Number of layers					
	3-layer	4-layer	5-layer	6-layer	7-layer	8-layer
Step 1	2	2	2	2	2	2
Step 2	3	3	3	3	3	3
Step 3	-	4	4	5	5	4
Step 4	-	-	-	-	-	7

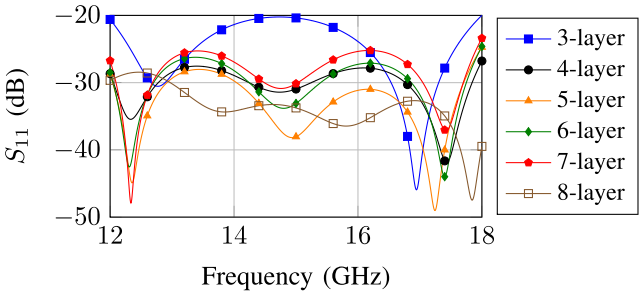

FIGURE 7. Simulation results of all the transitions at Ku-band.

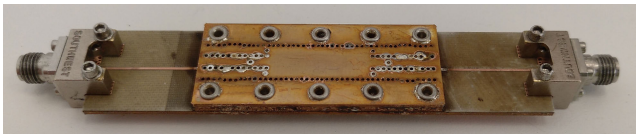

FIGURE 8. Fabricated prototype of the back-to-back transition from 1-layer height ESIW to 4-layer height ESIW.

All the designed transformers provide excellent results, which are very close to the performance expected for an ideal height transformer in classical rectangular waveguide.

IV. FREQUENCY SCALING

A full suite of transitions to increased height output ESIWs, ranging from 3 to 8 layers, has already been designed. The transitions have been implemented to operate at Ka-band, but the designs presented in this work can be easily transferred to other bands if the transition dimensions are properly scaled. To illustrate this, the original Ka transitions are mapped to Ku-band. The proposed frequency scaling works very well if the width/height ratio of the waveguides at the new band is close (not necessarily equal) to the original one. If this is not the case, the results of the scaling could be used as a good starting point of an optimization, identical to the one performed at the fifth step of the design process, that would refine the response of the transition.

The scaling factor we will use in order to translate the designed transitions from Ka-band to Ku-band is Coef $=$ $15.7988/7.112 = 2.2214$, the ratio between the waveguide widths at both bands (WR-62 and WR-28).

To obtain the scaled dimensions at Ku-band, the final dimensions for Ka-band listed in Table 3 are used. There is no need for re-optimizing the dimensions of the transition, since the substrate used for this implementation at Ku-band will be a Rogers 4003C substrate of height $h_c = 0.813$ mm, and the ratio with the former substrate ($h = 0.305$ mm) is quite close to the ratio of the scaled dimensions. The only structure that must be re-designed is the first part of the transition [9], that must be adapted to this new substrate and frequency band. The dimensions of the transformers at Ku-band, are listed in Table 4.

The results for these transformers at Ku-band are represented in Fig. 7 in the frequency range from 12 to 18 GHz. As advanced before, there is no need to re-optimize these transitions since they exhibit, after direct scaling, very good performance in terms of return loss.

V. RESULTS

Once the design procedure has been verified, a prototype of the back-to-back transition from 1-layer height ESIW to 4-layer height ESIW, as described in subsection III-B, has been fabricated at Ka-band in order to test its performance. The substrate employed to manufacture this prototype is a Rogers 4003C of height $h_c = 0.305$ mm, permittivity $\epsilon_r = 3.55$, and metal thickness $t = 26.5$ μm (considering both original and galvanic metallizations). Just to enclose the device, cover layers made of FR-4 of height $h = 1$ mm, with the same metallization, are used. FR-4, or any other plateable of metallic material could be used for the covers, since electromagnetic fields cannot penetrate the material. The rows of vias that can be seen in these covers, and also in the other layers (see figures 9(a) and 9(b)), have been manufactured in order to provide better soldering results (see [11] for more details). A photograph of the fabricated prototype is shown in Fig. 8.

A detail of the transition and a cross-section view of the manufactured device, showing the final structure, are also depicted in Fig. 9.

The measured results of the fabricated back-to-back prototype of the transition are represented in Fig. 10, and then compared to the simulated scattering parameters obtained with CST Microwave Studio in the frequency range from 26.5 to 40 GHz. We must remark that, in this case, the results incorporate the first part of the transition [9] that allows microstrip feedings. As can be seen, there is a reasonable good agreement between simulated and measured results. The degraded return loss, which in any case is above 10 dB in the whole frequency band, is due to the first part of the transition [9], which limits the performance of the whole transition.

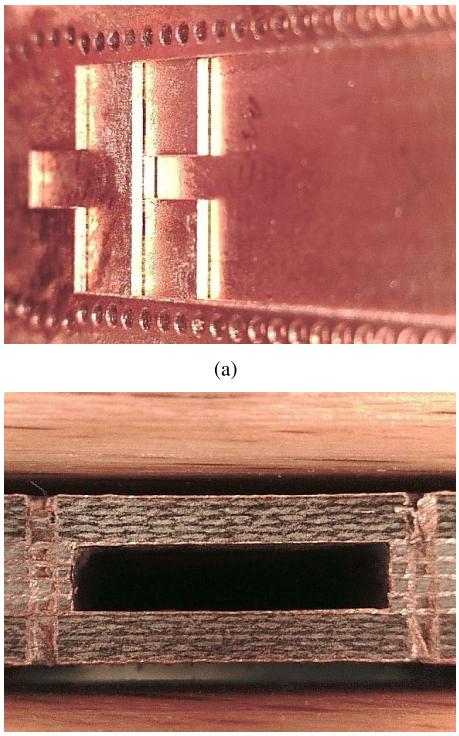

(a)

(b)

FIGURE 9. Manufactured device. (a) Detail of the transition, where rows of soldering vias have been mechanized to provide a better soldering finishing [11]. (b) Cross-section view.

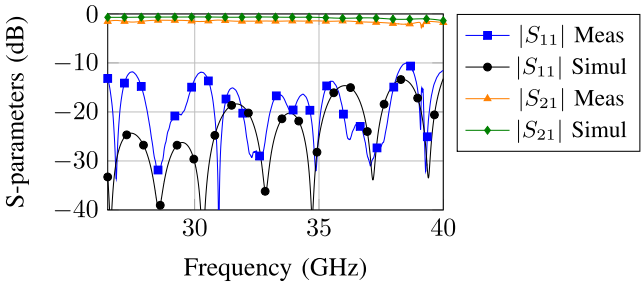

FIGURE 10. Comparison of measured and simulation results of the fabricated transition at Ka-band.

TABLE 5. Comparison between [8] and the wideband transition developed in this work. *The table has been made comparating the CST simulation results of both ESIW transitions (not including the microstrip transition).

	Transition of [8]	Wideband transition
FBW ($RL > 20\,dB$)*	10.9%	40.60%
Number of layers	$4, 9, 16 \cdots$	≥ 3
Losses	$0.046\,dB$	$0.069\,dB$
Lenght	$2.5085\,mm$	$5.8016 - 11.5139\,mm$

Therefore, the main advantage of the proposed design method has been shown, since notably good results have been achieved in the whole bandwidth, not only in a small range around the the central frequency as in [8].

Table 5 shows a comparison between the multilayer transition developed in [8], which is the only multilayer transition known at this time in this technology, and the wideband transition detailed in this paper. This new transtion provides a larger bandwidth of operation (covering the whole useful bandwidth of the waveguide), and it can be designed for any number of output layers greater than 3. This advantages are obtained at the cost of increasing the length of the transition, and its insertion loss (which is negligible in any case). The highlighted advantages, increased bandwidth and arbitrary number of output layers, make this new transition a very interesting alternative to increase the performance of ESIW technology at high frequencies.

VI. CONCLUSION

A new wideband transition that covers all the usable bandwidth for ESIWs of increased height is presented in this paper. First, a novel procedure for designing a structure for transitioning between multilayer ESIWs of different heights is described. The proposed design method can be adapted for different frequency bands, by simply scaling already optimized prototypes. To illustrate this property, a set of transitions designed to operate at Ka-band have been adapted to Ku-band, by simply scaling its dimensions.

A back-to-back prototype for this kind of transitions, operating at Ka-band, is successfully designed, fabricated, and measured. Experimental results have shown a good performance of the manufactured prototype. The main goal of this work has been achieved since a functional transition between ESIWs of different heights, which covers the whole bandwidth of the waveguides, has been experimentally validated. This new transition will allow to achieve the maximum performance and possibilities of ESIW technology, becoming a very important achievement for developing high quality devices operating at any frequency range.

REFERENCES

[1] D. Deslandes and K. Wu, "Integrated microstrip and rectangular waveguide in planar form," *IEEE Microw. Wireless Compon. Lett.*, vol. 11, no. 2, pp. 68–70, Feb. 2001.

[2] A. Belenguer, H. Esteban, and V. E. Boria, "Novel empty substrate integrated waveguide for high-performance microwave integrated circuits," *IEEE Trans. Microw. Theory Techn.*, vol. 62, no. 4, pp. 832–839, Apr. 2014.

[3] F. Parment, A. Ghiotto, T.-P. Vuong, J.-M. Duchamp, and K. Wu, "Broadband transition from dielectric-filled to air-filled substrate integrated waveguide for low loss and high power handling millimeter-wave substrate integrated circuits," in *IEEE MTT-S Int. Microw. Symp. Dig.*, Jun. 2014, pp. 1–3.

[4] F. Parment, A. Ghiotto, T. P. Vuong, J. M. Duchamp, and K. Wu, "Air-filled substrate integrated waveguide for low-loss and high power-handling millimeter-wave substrate integrated circuits," *IEEE Trans. Microw. Theory Techn.*, vol. 63, no. 4, pp. 1228–1238, Apr. 2015.

[5] A. Belenguer, A. L. Borja, H. Esteban, and V. E. Boria, "High-performance coplanar waveguide to empty substrate integrated coaxial line transition," *IEEE Trans. Microw. Theory Techn.*, vol. 63, no. 12, pp. 4027–4034, Dec. 2015.

[6] L. Jin, R. M. A. Lee, and I. Robertson, "Analysis and design of a novel low-loss hollow substrate integrated waveguide," *IEEE Trans. Microw. Theory Techn.*, vol. 62, no. 8, pp. 1616–1624, Aug. 2014.

[7] F. Bigelli, D. Mencarelli, M. Farina, G. Venanzoni, P. Scalmati, C. Renghini, and A. Morini, "Design and fabrication of a dielectricless substrate-integrated waveguide," *IEEE Trans. Compon., Packag., Manuf. Technol.*, vol. 6, no. 2, pp. 256–261, Feb. 2016.

[8] J. A. Martinez, J. J. de Dios, A. Belenguer, H. Esteban, and V. E. Boria, "Integration of a very high quality factor filter in empty substrate-integrated waveguide at *Q*-band," *IEEE Microw. Wireless Compon. Lett.*, vol. 28, no. 6, pp. 503–505, Jun. 2018.
[9] H. Esteban, A. Belenguer, J. R. Sánchez, C. Bachiller, and V. E. Boria, "Improved low reflection transition from microstrip line to empty substrate-integrated waveguide," *IEEE Microw. Wireless Compon. Lett.*, vol. 27, no. 8, pp. 685–687, Aug. 2017.
[10] C. S. Gledhill and A. M. H. Lssa, "Exact Solutions of Stepped Impedance Transformers Having Maximally Flat and Chebyshev Characteristics," *IEEE Trans. Microw. Theory Techn.*, vol. 17, no. 7, pp. 379–386, Jul. 1969.
[11] J. A. Martinez, A. Belenguer, and H. Esteban, "Highly reliable and repeatable soldering technique for assembling empty substrate integrated waveguide devices," *IEEE Trans. Compon., Packag., Manuf. Technol.*, to be published.

JUAN A. MARTÍNEZ received the telecommunications engineering degree from the University of Castilla-La Mancha (UCLM), Cuenca, Spain, in 2012, and the master's degree in research telecommunications (electronics and communications specialized) from the University Miguel Hernandez (UMH), Elche, Spain, in 2013. In 2013, he joined the University of Castilla-La Mancha, where he was with the Grupo de Electromagnetismo Aplicado, as a Research Assistant. His research interests include computational electromagnetics, analysis and synthesis of passive microwave circuits and antennas, and SIW devices analysis and their applications.

ANGEL BELENGUER (M'04–SM'14) received the degree in telecommunications engineering and the Ph.D. degree from the Universidad Politècnica de Valencia (UPV), Spain, in 2000 and 2009, respectively. He joined the Universidad de Castilla-La Mancha, in 2000, where he is currently a Profesor Titular de Universidad with the Departamento de Ingeniería Eléctrica, Electrónica, Automática y Comunicaciones. He has authored or coauthored more than 50 articles in peer-reviewed international journals and conference proceedings and frequently acts as a reviewer for several international technical publications. His research interests include methods in the frequency domain for the full-wave analysis of open-space and guided multiple scattering problems, EM metamaterials, and empty substrate integrated waveguide (ESIW) devices and their applications.

JUAN J. DE DIOS received the Ingeniero de Telecomunicación degree and the Doctor Ingeniero de Telecomunicación degree (Ph.D. degree in Communications) *(summa cum laude)* from the E.T.S. Ingenieros de Telecomunicación, Universidad Politécnica de Madrid, Spain, in 1991 and 2004, respectively. He was with Lucent Technologies (formerly AT&T) at Transmission Engineering Lab (Bell Labs), Madrid, Spain, from 1991 to 1999. Since 1999, he has been with the Escuela Politécnica de Cuenca, Universidad de Castilla-La Mancha, Spain, where he is currently a Professor Titular de Universidad with the Departamento de Ingeniería Eléctrica, Electrónica, Automática y Comunicaciones. His research interests include image and video processing, RFID, microwave circuits and antennas, and SIW devices analysis and their applications.

HÉCTOR ESTEBAN GONZÁLEZ (S'03–M'99–SM'14) received the degree in telecommunications engineering and the Ph.D. degree from the Universidad Politècnica de Valencia (UPV), Spain, in 1996 and 2002, respectively. He was with the Joint Research Centre, European Commission, Ispra, Italy. In 1997, he was with the European Topic Centre on Soil (European Environment Agency). He rejoined the UPV, in 1998. His research topics have included methods for the full-wave analysis of open-space and guided multiple scattering problems, CAD design of microwave devices, electromagnetic characterization of dielectric and magnetic bodies, and the acceleration of electromagnetic analysis methods using the wavelets and FMM. He is currently focused on the development of substrate integrated devices.

VICENTE E. BORIA (S'91–A'99–SM'02–F'18) was born in Valencia, Spain, in May 1970. He received the Ingeniero de Telecomunicación degree (Hons.) and the Doctor Ingeniero de Telecomunicación degree from the Universidad Politècnica de Valencia, Valencia, Spain, in 1993 and 1997, respectively. In 1993, he joined the Departamento de Comunicaciones, Universidad Politècnica de Valencia, where he has been a Full Professor, since 2003. From 1995 to 1996, he was holding a spanish trainee position with the European Space Research and Technology Centre, European Space Agency (ESTEC-ESA), Noordwijk, The Netherlands, where he was involved in the area of EM analysis and design of passive waveguide devices. He has authored or coauthored ten chapters in technical textbooks, 180 articles in refereed international technical journals, and more than 200 papers in international conference proceedings. His current research interests are focused on the analysis and automated design of passive components, left-handed and periodic structures, as well as on the simulation and measurement of power effects in passive waveguide systems. He is a member of the Technical Committees of the IEEE-MTT International Microwave Symposium and the European Microwave Conference. He has also been a member of the IEEE Microwave Theory and Techniques Society (IEEE MTT-S) and the IEEE Antennas and Propagation Society (IEEE AP-S), since 1992. He acts as a regular reviewer of the most relevant IEEE and IET technical journals on his areas of interest. He has been an Associate Editor of the IEEE Microwave and Wireless Components Letters, from 2013 to 2018, and *IET Electronics Letters*, from 2015 to 2018. He currently serves as a Subject Editor (Microwaves) of *IET Electronics Letters*, and as an Editorial Board member of *International Journal of RF and Microwave Computer-Aided Engineering*.